
MODELING AND DETERMINATION OF OPTIMAL SWITCHING ANGLES FOR SWITCHED RELUCTANCE MOTOR DRIVES

Karthik.V and V.V.Narsimha Murthy

M-tech Student scholar , University College of engineering, Jntu Kakinada.
Associate Professor , University college of engineering, Jntu kakinada.

Abstract

We present a lookup table based model for switched reluctance motors (SRMs). The model uses four coefficients, which are rotor position dependent and calculated from the flux-current-angle data using curve fitting. The four coefficients are further represented with sixth degree polynomials, which can be calculated effectively with Qin Jiushao's method. Simulated results show that the magnetic characteristics calculated with our model agree well with the original flux-current-angle data. Also a method is proposed to produce optimal switching angles, based on a non-linear inductance model of low inductance region for switched reluctance motor (SRM). The optimal turn-on angle is derived from the non-linear model and electrical equation of SRM while optimal turn-off angle is derived from the turn-on angle. The proposed method has more accuracy than the conventional analytical method and improves the efficiency of the drive. Simulation results demonstrate the validity and effectiveness of the proposed method.

KEY WORDS:

Modeling and determination , Motor Drives , switched reluctance motors .

INTRODUCTION

SWITCHED reluctance motors (SRMs) provide many structural advantages, such as rigidity, brushless, less maintenance, low cost, etc. Furthermore, since the rotor of the SRM does not generate significant heat, the motor is easy to cool thereby allowing the SRM to be employed in high-temperature and harsh operating environments. All these merits of the SRM have caused it to draw great attention from industry and researchers as an alternative among other electrical machines in the applications of hybrid electric vehicles, windmill generators, household appliances, and aircraft. Due to the effects of saturation, hysteresis, and the double saliency of the machine construction, the SRM magnetic characteristics are of high nonlinearity and are difficult to model. The magnetic characteristics of an SRM can be taken into account by appropriate modeling of the nonlinear flux-current-angle characteristics in one phase of the machine. The machine model may then be described by

$$\Psi = \Psi(i, \theta) \quad (1)$$

Where Ψ is flux linkage, i is phase current and θ is rotor position.

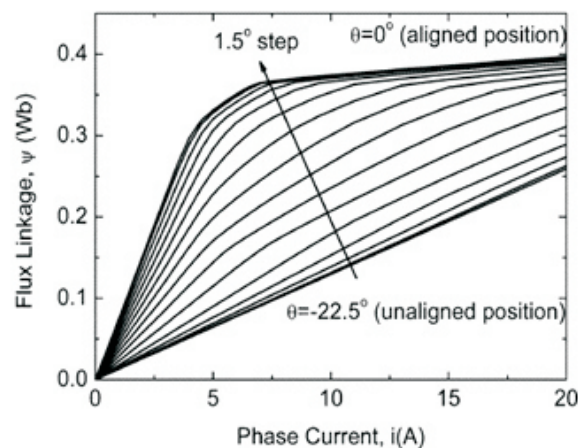


Fig. 1. Flux linkage versus phase current with different rotor positions for a 12/8 SRM.

Analytical models can be derived either from the machine geometry and magnetic theory directly or from the previously obtained $\Psi(i, \theta)$ data using numerical methods. For the analytical models development, one of the popularly used methods is to fit the previously obtained $\Psi(i, \theta)$ data with analytical equations.

In this paper, a simple model by fitting the previously obtained $\Psi(i, \theta)$ data with analytical equations is presented. The electromagnetic torque, which is denoted by $T(i, \theta)$, further calculated from the proposed $\Psi(i, \theta)$. The validity of this model has been verified through simulation and the results show that the proposed method is effective and accurate.

A large number of methods for optimising turn-on angle and turn-off angle have been presented during past years, which can be approximately classified as following: artificial intelligence method, self-tuning method and analytical method.

In the following two papers, artificial intelligence method is applied. To maximise the torque per ampere at all operating points, [3] presents a control strategy which is based on neural network taking reference current and speed as inputs and turn-on angle and turn-off angle as outputs. In [4], the turn-on angle and turn-off angle are optimised by an adaptive neuro-fuzzy controller which combines the expert knowledge of the fuzzy inference system and the learning capability of neural networks.

Self-tuning method is more widely discussed. Torrey and Lang [5] present an algorithm to determine the optimal turn-on angle and turn-off angle, which is based on the determination of local optimum at each operating point for each possible number of chops in the current waveform. In [6], the duty rate of the applied DC voltage is varied in order to obtain the desired speed quickly, and then the turn-on angle is varied step by step to minimise the energy consumption when operating in a steady-state. A new approach to the automatic control of the turn-on angle is presented to increase the maximum torque per ampere in [7], where a closed-loop control algorithm is designed to adjust turn-on angle which ensures that the first peak of the phase current occurs at the angle where the rotor poles begin to overlap the stator poles. The method requires comparing the phase current with the reference current and also needs a shaft encoder to detect the position of the first peak of the phase current continuously. Based on the previous work in [7, 8] it adds automatic control of the turn-off angle to maximise system efficiency. The relationship between speed, reference current and optimised turn-off angle are obtained through experiment. Then, curve fitting is applied to deduce the formula of the optimised turn-off angle. However, it needs to traverse all the possible turn-off angles.

Considering that the self-tuning method has potential

complication when being implemented, the analytical method is also widely used in optimisation control because of its simplicity of structure in application. The conventional model is also applied to deduce formulae of turn-on angle and turn-off angle in [9]. However, the maximum inductance used in the formulae differs greatly in different phase current conditions, leading to a

decreased accuracy on optimal turn-on angle and turn-off angle. As discussed in [10], an initial turn-on angle is given by the conventional analytical method. Within a certain range around the initial value, an experiment is conducted to find a set of angles with the highest efficiency. The conventional analytical method based on the linear inductance model starts to break down as back electromotive force (EMF) voltage becomes prominent especially at high speed.

This paper proposes an improved analytical method to provide analytical formulae to calculate the optimal turn-on angle and turn-off angle which can be applied both at low speed and high speed. The method is based on a non-linear model of inductance only in the low inductance region. The optimal turn-on angle makes the first peak phase current reach reference current when the rotor reaches a position where the rotor poles begin to overlap the stator poles. The optimal turn-off angle ensures that phase current decays to zero before the motor reaches the negative torque region. The efficiencies are improved with the proposed method. Simulation results demonstrate the validity and effectiveness of the proposed method.

MODEL DEVELOPMENT

A. Flux Linkage-Current Relation

It can be seen from Fig. 1 that saturation is one of the most important properties of the $\psi - i$ curves, especially at the aligned position. Due to the inherent property of the exponential function, both the models in [11] and [12] are difficult to capture the severe curvature of the $\psi - i$ curve at the aligned position. In this paper, we model the $\psi - i$ curve for each rotor position as

$$\Psi = f_1 i + f_2 \tag{2}$$

Where f_1 and f_2 are phase current i dependent variables. It is obvious that both f_1 and f_2 should exhibit the saturation property when i is greater than the threshold saturated current. In this work, both f_1 and f_2 are defined in the form of Gaussian function

$$f_1 = a_2 e^{-\left(\frac{i}{a_1}\right)^2} + a_3 \tag{3}$$

$$f_2 = a_4 e^{-\left(\frac{i}{a_2}\right)^2} - a_1 \tag{4}$$

Where a_1, a_2, a_3 and a_4 are constant coefficients for a given rotor position.

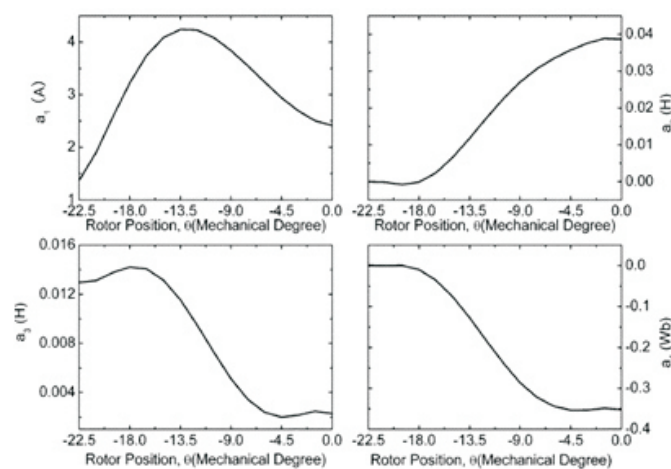


Fig. 2. Coefficients $a_1, a_2, a_3,$ and a_4 as functions of the rotor position θ .

TABLE I
POLYNOMIAL COEFFICIENTS USED TO REPRESENT THE FITTING
COEFFICIENTS IN (6)

	a_{m-1} (A)	a_{m-2} (H)	a_{m-3} (H)	a_{m-4} (Wb)
c_{m0}	2.4159822e+0	3.8667577e-2	2.2785122e-3	-3.5128437e-1
c_{m1}	-1.0913682e+0	-5.4588670e-2	-2.8853825e-2	-3.6245932e-1
c_{m2}	9.8199489e+1	-2.3904244e+0	-1.0909303e+0	-1.3032807e+1
c_{m3}	4.4137610e+2	-2.4541631e+1	-1.1135325e+1	-1.1892130e+2
c_{m4}	1.8033592e+3	-1.4262150e+2	-3.4481244e+1	-1.6076961e+2
c_{m5}	7.3725381e+3	-3.7239578e+2	-3.1121778e+1	4.9568484e+2
c_{m6}	9.8370905e+3	-3.4461566e+2	6.1686322e+0	9.4612459e+2

Substituting (3) and (4) into (2) yields

$$\Psi = \left(a_2 e^{-\left(\frac{i}{a_1}\right)^2} + a_3 \right) i + a_4 e^{-\left(\frac{i}{a_1}\right)^2} - a_4 \quad (5)$$

The coefficients a_1 , a_2 , a_3 and a_4 can be calculated through the $\psi - i - \theta$ data using numerical curve fitting. In this work, all these coefficients are represented by sixth degree polynomials.

$$a_m = \sum_{j=0}^6 C_{mj} \theta^j \quad m=1, 2, 3, 4 \quad (6)$$

Where C_{mj} is the j th coefficient in the polynomial representing a_m

Now for a given rotor position θ and phase current i the corresponding flux linkage ψ can be calculated with (5) and (6).

B. Torque Production

The electromagnetic torque of phase j can be determined according to

$$T_j = \frac{\partial}{\partial \theta} \int_{i_0}^i \Psi_j dx \quad (7)$$

Substituting (5) into (7) yields

$$T_j = \left(a_1 a_2 \frac{da_1}{d\theta} + \frac{a_1^2}{2} \frac{da_2}{d\theta} \right) \left[1 - e^{-\left(\frac{i}{a_1}\right)^2} \right] - \left(a_2 i + a_4 \right) \frac{i}{a_1} \frac{da_1}{d\theta} e^{-\left(\frac{i}{a_1}\right)^2} + \frac{\sqrt{\pi}}{2} \left(a_1 \frac{da_1}{d\theta} + a_1 \frac{da_4}{d\theta} \right) \operatorname{erf} \left(\frac{i}{a_1} \right) + \frac{i^2}{2} \frac{da_3}{d\theta} - i \frac{da_4}{d\theta} \quad (8)$$

where the derivative terms $\frac{da_j}{d\theta}$ ($j=1,2,3,4$) can be derived from (7), and $\operatorname{erf}(x)$ is the error function which is defined by

$$\operatorname{erf}(x) = \frac{2}{\sqrt{\pi}} \int_0^x e^{-t^2} dt \quad (9)$$

Note that $\operatorname{erf}(x)$ is nonintegrable. To solve this problem, we used the hyperbolic tangent function $\tanh(kx)$ to approximate $\operatorname{erf}(x)$ well with the coefficient k very close to 1.2027825.

C. Low inductance region

The objectives of the proposed method can be explained through the relationship between the idealised inductance and the typical idealised phase current waveform for a 12/8 SRM as shown in Fig.

3. The electrical period is 45° and the unaligned angle θ_u is defined as -22.5° , whereas the aligned angle θ_a is 0°

The maximum power is produced when the first peak current occurs at the angle marked θ_0 in Fig. 3, namely that maximum torque per ampere occurs as the rotor poles begin to overlap the stator poles. Therefore the phase winding must be turned on before θ_0 to make sure that the first peak current is at reference current I_{ref} when the rotor reaches θ_0 .

The low-inductance region is defined as the angular interval over which the rotor poles do not overlap the stator poles, as shown in Fig. 3 from the unaligned angle θ_u to θ_a . In order to find the optimal turn-on angle, the process of phase current rising from zero to I_{ref} needs to be analysed.

Fig. 4 shows the influence on phase current in the case of the actual and idealised phase inductance. As is depicted, the linear inductance model using idealised phase inductance, assumes that the inductance remains unchanged in the low-inductance region and ignores the relationship between inductance and rotor position, neglecting the back EMF voltage. Actually, in the low-inductance region, the inductance is not constant and its non-linearity has a significant influence on the actual phase current waveform, leaving the turn-on angle θ_{on} different from that of the ideal condition. In the actual inductance condition, considering the back EMF, the turn-on angle calculated is advanced. For the different turn-on angles, the values of phase currents' first peaks differ a lot (Δi) in high speed operation and that the positions of phase currents' first peaks differ a lot ($\Delta \theta$) in low speed operation.

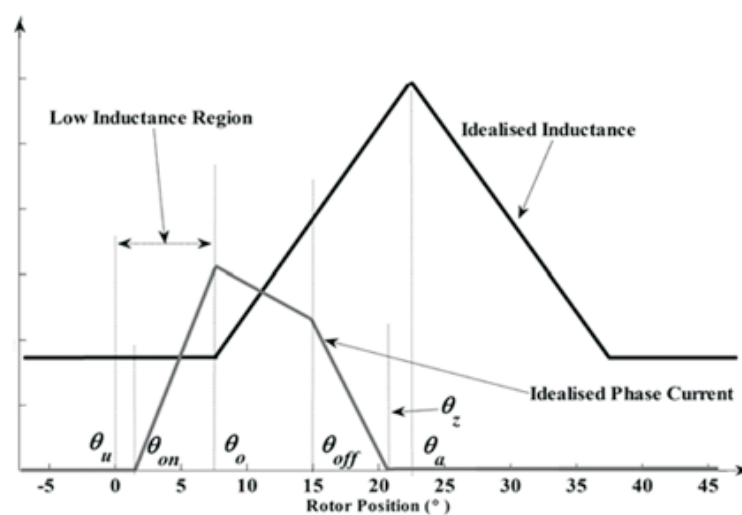


Fig. 3 Idealised phase inductance against rotor position with typical idealised phase current waveform showing different angles

Consequently, when analysing the process of phase current rising in the low-inductance region, non-linearity should be taken into account. In view of this, a non-linear model of the low-inductance region is required and there is no need to model the phase inductance of the whole region.

Fig. 5a shows the phase inductance against rotor position with different phase current. The influence of current on the inductance differs around θ_0 . That is, phase current has a great impact on inductance after θ_0 whereas it has little influence on inductance before θ_0 as shown in Fig. 5b. In the low-inductance region, the minimum value of $dL/d\theta$ is $3.7e-6$, much larger than the maximum value of dL/di , $7.1e-8$. This means the effect of current can be ignored in a low-inductance region. From the shape of phase inductance in the low-inductance region, the phase inductance changes exponentially with rotor position, so the relationship between inductance and position in the low-inductance region can be written as

$$L = a * e^{\frac{(\theta-b)}{c}} \tag{10}$$

where L is the inductance, θ is the rotor position and a, b, c are parameters, which can be determined

through curve fitting.

D. Defining the optimal turn-on angle

To optimise the turn-on angle which ensures the first peak of the phase current to occur at θ_0 the time during which the phase current changes from zero to peak at an assumed constant speed should be deduced first. Namely that, the relationship between current i and time t should be figured out first.

The electrical equation of SRM can be described as follows

$$V_s = Ri + L(\theta) \frac{di}{dt} + i\omega \frac{dL(\theta)}{d\theta} \tag{11}$$

where V_s is the source voltage, R is the phase resistance, L represents the inductance, i denotes the phase current and ω is the rotor speed. The first term of (11) is the resistance drop, while the second term is the induced EMF voltage caused by variation of current, and the third term is the back EMF voltage caused by rotor position change.

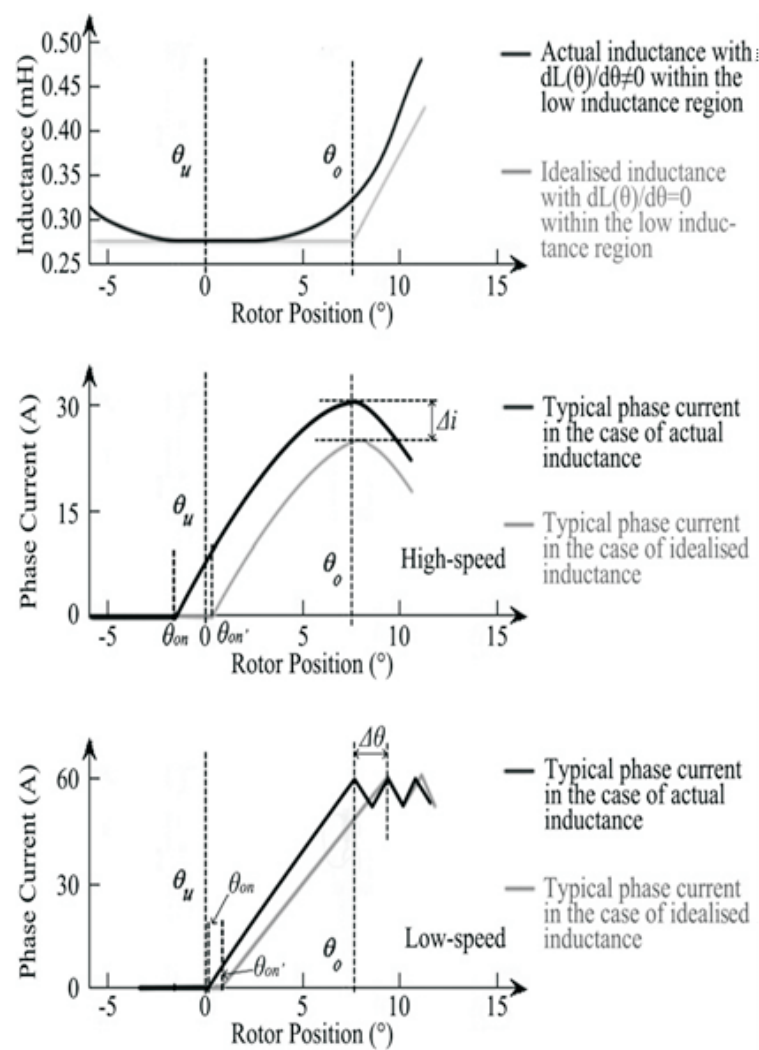


Fig. 4 Actual and idealised inductance against rotor position with typical phase current waveform

In conventional analytical method, the turn-on angle θ_{on} is given as

$$\theta_{on} = \theta_c - \frac{\omega L_{min} I_{ref}}{V_s} \tag{12}$$

where L_{min} is the minimum inductance, I_{ref} is the reference current, θ_0 is decided by stator pole arc and rotor pole arc, which are parameters of SRM structure.

Equation (12) assumes that the inductance is constant within the low-inductance region $[\theta_u, \theta_0]$ then the third term of (11), back EMF voltage, is zero and has been omitted. Therefore the conventional analytical method starts to break down as back-EMF voltage becomes prominent especially at high speed. With these facts, it is necessary to have a new formula taking back-EMF voltage into consideration.

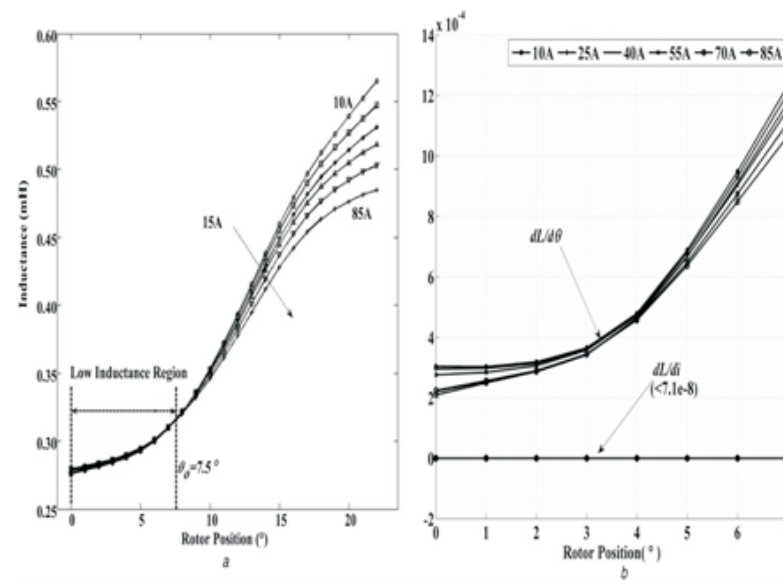


Fig. 5 Inductance and effect of current rotor position
 a Inductance against rotor position with different phase current
 b Effect of current and rotor position on inductance in low-inductance region

In order to deduce the new formula, (11) can be rewritten as follows

$$V_s = L(\theta) \frac{di}{dt} + i \left(R + \frac{dL(\theta)}{d\theta} \omega \right) \quad (13)$$

Solving the equation about I, yields

$$i(t) = \frac{V_s}{R + \omega \left(\frac{dL}{d\theta} \right)} + \left[I_0 - \frac{V_s}{R + \omega \left(\frac{dL}{d\theta} \right)} \right] e^{-t/\tau} \quad (14)$$

Where τ

$$\tau = \frac{L(\theta)}{R + \omega \left(\frac{dL}{d\theta} \right)} \quad (15)$$

Before the phase is turned on, the current is zero. Therefore $I_0=0$ One thing that must be pointed out is that in this case

$$R \ll \omega \left(\frac{dL}{d\theta} \right) \quad (16)$$

The resistance of the phase winding when compared with the rotor speed ω multiplied by change rate of inductance, it can be omitted.

When rotor reaches θ_0 from θ , the current reaches its peak as shown in Fig. 3. We can obtain the time between θ and θ_0 as follows

$$t = \frac{\theta_0 - \theta}{\omega} \quad (17)$$

Substituting (15)–(17) into (14)

$$\frac{i\omega}{V_s} \frac{dI}{d\theta} = 1 - e^{\left(\frac{i\theta - \theta_0}{L}\right) \left(\frac{dL}{d\theta}\right)}$$

So current function of time $i(t)$ is converted into current function of angle $i(\theta)$ substitute (10) into (18), θ is the optimal turn-on angle and can be rewritten as

$$\theta_{on} = \theta_0 - \ln\left(1 - \frac{a\omega i}{cV_s} e^{-(b-\theta_0)/c}\right) \quad (19)$$

where i is the commanded phase current when the rotor reaches θ_0 . Here, it is reference current I_{ref} . The other parameters a, b, c are obtained in (10) through the curve fitting method.

This formula considers back EMF, so it provides optimal turn-on angle over a wide speed range. Owing to its analytical nature, the proposed formula has fast constringency and there is no need of either continuously monitoring the position of the first peak of phase current or detecting other special parameters for feedback.

E. Defining the optimal turn-off angle

Fig. 6 shows that when phase winding is turned on, the phase voltage is positive and the flux-linkage starts to rise up from zero, reaching the peak at θ_{off} . When the phase winding is turned off, the phase voltage is negative and the fluxlinkage starts to fall down. When the current decays to zero, flux-linkage decays to zero as well, so is the phase voltage. Flux-linkage is the integral of phase voltage for time

$$\Psi = \int (V_s - iR)dt \quad (20)$$

then the flux-linkage as Fig. 6 shows can be represented as

$$(V_s - iR)t_{up} + (-V_s - iR)t_{down} = 0 \quad (21)$$

Where t_{up} is the flux-linkage's rising time and t_{down} is its falling time.

$$t_{up} = \frac{\theta_{off} - \theta_{on}}{\omega} \quad (22)$$

$$t_{down} = \frac{\theta_z - \theta_{off}}{\omega} \quad (23)$$

Assume

$$iR \ll V_s \quad (24)$$

hence, iR can be omitted. Substitute (22),(23),(24) into (21) and it is easy to obtain:

$$\frac{\theta_{off} - \theta_{on}}{\omega} V_s = \frac{\theta_z - \theta_{off}}{\omega} V_s \quad (25)$$

So,
$$\theta_{off} = \frac{\theta_z - \theta_{on}}{2} \quad (26)$$

In the equation above, θ_z represents the very position where the phase current decays to zero. In order to avoid negative torque and make sure that the phase current decays to zero before the aligned angle θ_z was set as θ_a

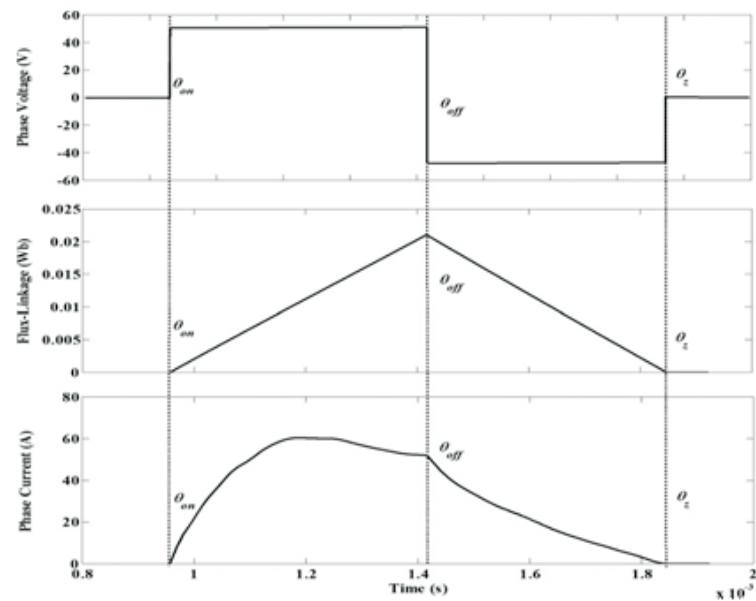


Fig. 6 Flux-linkage against phase current in an electrical period

MODEL SIMULATION AND RESULTS

Matlab/Simulink was used to perform the simulations with the presented model. For ease of the dynamic simulation, the following assumptions are made:

- i) dc-link voltage Vdc is constant;
- ii) converter is ideal;
- iii) mutual inductances, eddy current, and hysteresis effects of the SRM are neglectable.

The simulation block diagram is shown in Fig. 7. The commutation logic generates gating pulses for the converter. For the purpose of simulation, the phase current i needs to be solved according to flux linkage ψ and rotor position θ and thus we obtain the flux linkage-current-rotor position data. And also by using the torque expression given in equation (8) the torque profile can be obtained. Thus the current and torque data obtained are used in developing the simulink model of the SRM.

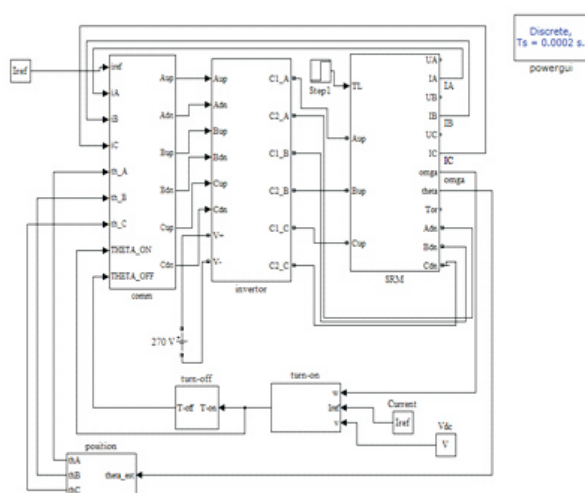


Fig 7 Simulink Block Diagram of SRM

Fig. 7 shows a block diagram of the SRM drive system using Matlab/Simulink. Turn-on angle controller using (19) makes I_{ref} and rotor speed as inputs and θ_{on} as output. Turn-off angle controller using (26) makes θ_{on} as input and θ_{off} as output.

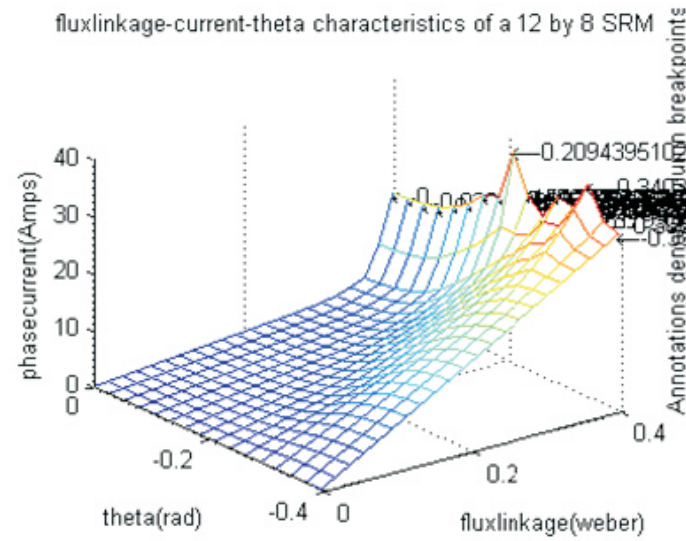


Fig.8 ψ - i - θ characteristics of SRM simulink model with Rotor position -22.5 deg (unaligned) to 0 deg (aligned).

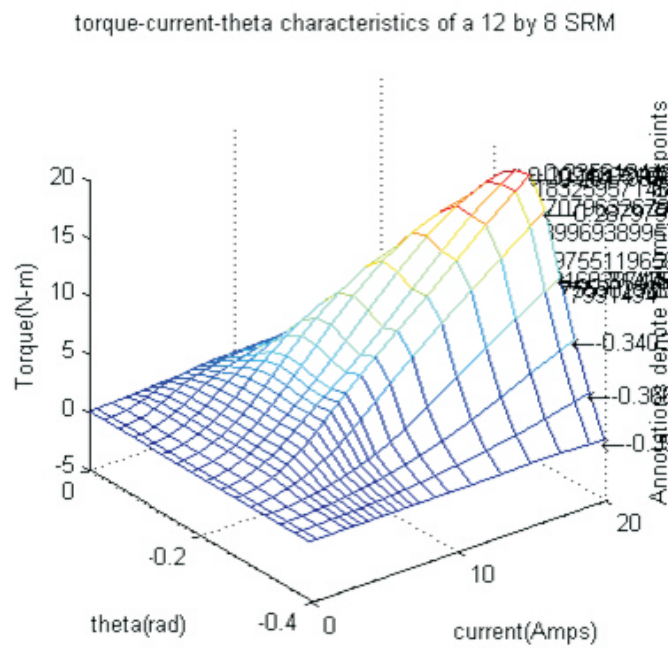


Fig.9 T- i - θ characteristics of the SRM simulink model.

Fig.8 and Fig.9 shows the (ψ - i - θ) and (T- i - θ) characteristics of the developed simulink model.

Fig.10 and Fig.11 shows the simulated phase current waveforms when the SRM runs with a speed of 1000r/m and 3200r/m.

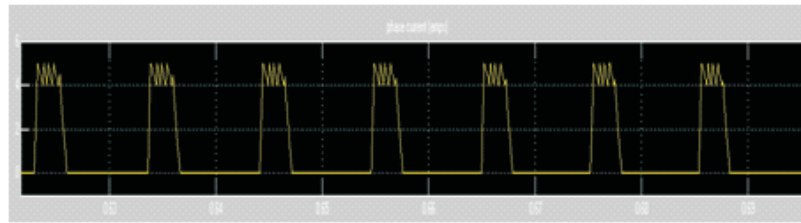


Fig.10 simulated phase current for no-load operation at 1000r/m.

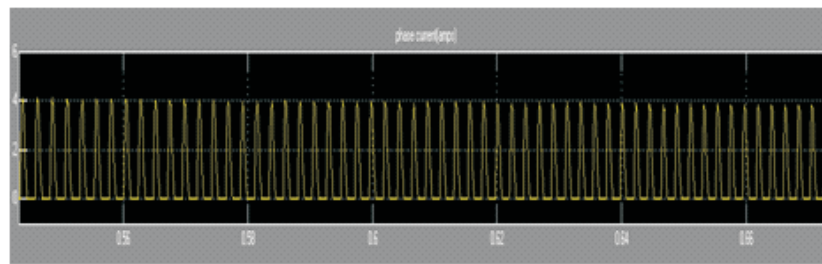
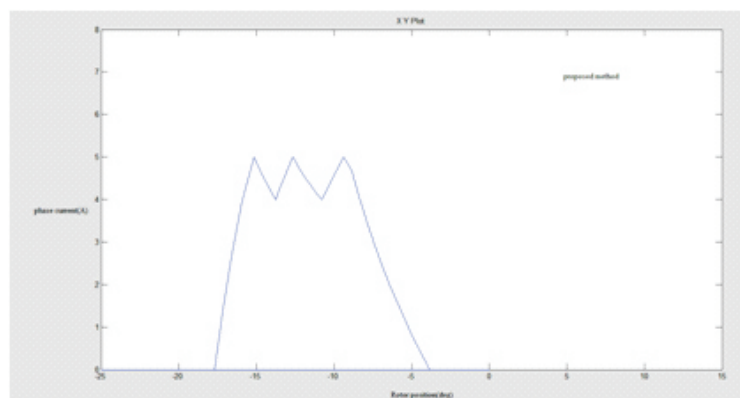
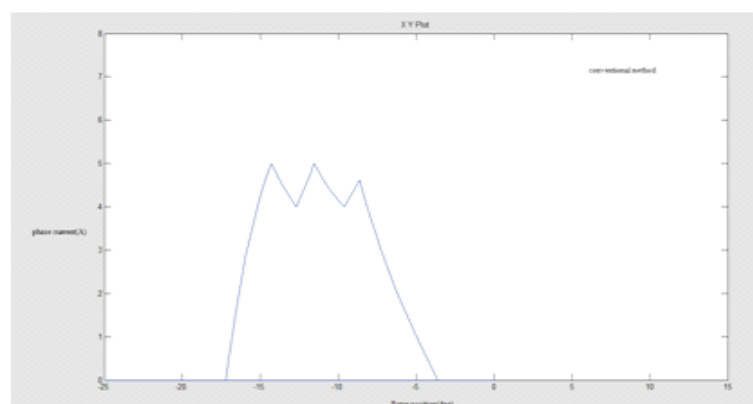


Fig.11 simulated phase current for no-load operation at 3200r/m.

Using the turn-on and turn-off angle controllers the optimal switching angles for the phase excitation are given. Fig. 12 (a) and Fig. 12 (b) show the simulated waveforms of the phase current versus rotor position using the proposed and conventional method respectively at low speed. we observe that in the proposed the first peak of the phase current is occurring at the position where the rotor and stator poles begin to overlap.



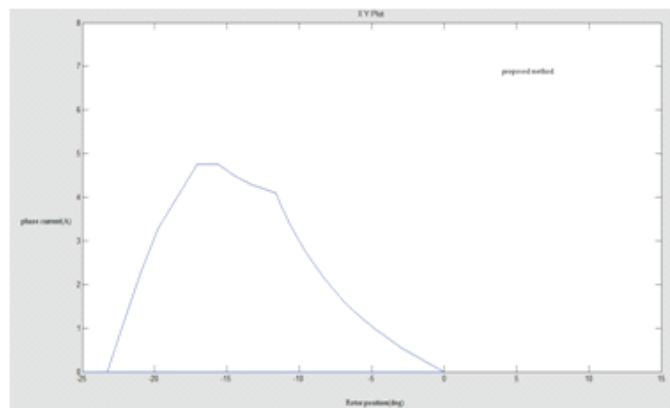
(a)



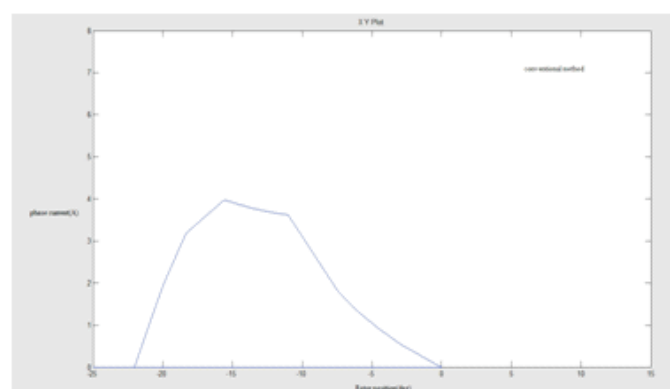
(b)

Fig.12 comparison of the current waveforms with the proposed and conventional method at 1000 rev/min.

Fig.13 (a) and Fig.13 (b) show the simulated waveforms of the phase current versus rotor position using the proposed and conventional method respectively at high speed.



(a)



(b)

Fig.13 comparison of the current waveforms with the proposed and conventional method at 3200 rev/min.

IV. CONCLUSIONS

This paper has presented a lookup table based SRM model. The validity of the model has been verified with the simulation results obtained compared with the experimental results given in the reference paper. Also a method that determines the optimal switching angles for SRM model is implemented using the turn-on and turn-off angle controllers.

The proposed method makes the first peak of the phase current at reference current when the rotor reaches the position where the rotor poles begin to overlap the stator poles resulting in higher torque and there by obtaining maximum power output. Comparisons of the conventional and proposed methods through simulations demonstrate the validity and effectiveness of the proposed method.

REFERENCES

1. Y.Z.xu, R.Zhong, L.Chen, S.L.Lu 'Analytical method to optimise turn-on angle and turn-off angle for switched reluctance motor drives
2. Chen, H.J., Jiang, D.Q., Yang, J., Shi, L.X.: 'A new analytical model for switched reluctance motors', IEEE Trans. Magn., 2009, 45, (8), pp. 3107–3113

3. Fahimi, B., Suresh, G., Johnson, J.P., Ehsani, M., Arefeen, M., Panahi, I.: 'Self-tuning control of switched reluctance motors for optimized torque per ampere at all operating points'. Proc. IEEE APEC'98, 1998, pp. 778–783
4. Beno, M.M., Marimuthu, N.S., Singh, N.A.: 'Improving power factor in switched reluctance motor drive system by optimising the switching angles'. TENCON 2008-2008 IEEE Region 10 Conf., pp. 1–5
5. Torrey, D.A., Lang, J.H.: 'Optimal-efficiency excitation of variable reluctance motor drives', Electr. Power Appl., IEE Proc. B, 1991, 138, (1), pp. 1–14
6. Kjaer, P.C., Nielsen, P., Andersen, L., Blaabjerg, F.: 'A new energy optimizing control strategy for switched reluctance motors', IEEE Trans. Ind. Appl., 1995, 31, (5), pp. 1088–1095
7. Sozer, Y., Torrey, D.A., Mese, E.: 'Automatic control of excitation parameters for switched-reluctance motor drives', IEEE Trans. Power Electron., 2003, 18, (2), pp. 594–603
8. Sozer, Y., Torrey, D.A.: 'Optimal turn-off angle control in the face of automatic turn-on angle control for switched-reluctance motors', IET Electr. Power Appl., 2007, 1, (3), pp. 395–401
9. Mademlis, C., Kioskeridis, I.: 'Performance optimization in switched reluctance motor drives with online commutation angle control', IEEE Trans. Energy Convers., 2003, 18, (3), pp. 448–457
10. Fatemi, S.A., Cheshmehbeigi, H.M., Afjei, E.: 'Self-tuning approach to optimization of excitation angles for switched-reluctance motor drives'. European Conf. on Circuit Theory and Design, 2009, pp. 851–856
11. Kim, J., Krishnan, R.: 'High efficiency single-pulse controlled switched reluctance motor drive for high speed (48k RPM) application: analysis, design, and experimental verification'. IEEE Industry Applications Society Annual Meeting, 2008
12. S. A. Hossain and I. Husain, "A geometry based simplified analytical model of switched reluctance machines for real-time controller implementation," IEEE Trans. Power Electron., vol. 18, no. 6, pp. 1384–1389, Nov. 2003.
13. A. D. Cheok and Z. Wang, "Fuzzy logic rotor position estimation based switched reluctance motor DSP drive with accuracy enhancement," IEEE Trans. Power Electron., vol. 20, no. 4, pp. 908–921, Jul. 2005.
14. W. Lu, A. Keyhani, and A. Fardoun, "Neural network-based modelling and parameter identification of switched reluctance motors," IEEE Trans. Energy Convers., vol. 18, no. 2, pp. 284–290, Jun. 2003.
15. Z. Y. Lin, D. S. Reay, B.W. Williams, and X. N. He, "Online modelling for switched reluctance motors using B-spline neural networks," IEEE Trans. Ind. Electron., vol. 54, no. 6, pp. 3317–3322, Dec. 2007.
16. A. Radun, "Analytically computing the flux linked by a switched reluctance motor phase when the stator and rotor poles overlap," IEEE Trans. Magn., vol. 36, no. 4, pp. 1996–2003, Jul. 2000.
17. A. Radun, "Analytical calculation of the switched reluctance motor's unaligned inductance," IEEE Trans. Magn., vol. 35, no. 6, pp. 4473–4481, Nov. 1999.